Structure and stability of Al-doped small Na clusters: Na_nAl ($n=1,10$)

Ajeeta Dhavale,* Vaishali Shah,† D. G. Kanhere†
Department of Physics, University of Pune, Pune 411 007, India
(Received 1 April 1997; revised manuscript received 29 October 1997)

We have investigated the ground-state geometries of aluminum-doped sodium clusters Na_nAl ($n=1,10$) using an *ab initio* molecular-dynamics method. It is seen that a single Al impurity atom affects significantly the geometries of small Na_n ($n\leqslant 6$) clusters, whereas the effect is less pronounced for large clusters. Our results show an early appearance of nonplanar ground-state geometries and it is observed that for $n\geqslant 6$ the Al atom gets trapped inside the Na cage. The stability of these clusters has been examined from the systematic analysis of energetics. This indicates Na_5Al and Na_7Al having 8 and 10 valence electrons to be the stable clusters. [S1050-2947(98)11306-9]

PACS number(s): 36.40.Qv, 36.40.Mr, 61.46.+w, 31.15.Ar

I. INTRODUCTION

The ground-state geometries, energetics, stability, and such other properties of clusters is currently the subject of intensive experimental and theoretical investigation [1,2]. The interest in the physics and chemistry of clusters arises due to a number of reasons such as the availability of free cluster sources, their distinct shapes, and characteristic electronic properties, which are different from bulk and the possibility of using them as building blocks for novel nanostructured materials, etc. The field of clusters has witnessed considerable growth in both experimental and theoretical understanding. A number of theoretical investigations using the powerful technique of density functional theory along with Car-Parrinello molecular dynamics [3] (CPMD) have been carried out. Such investigations have yielded valuable information about their structural, electronic, magnetic and optical properties.

By and large homoatomic clusters of Na [4], Mg [5], Al [6], P [7], Se [8], etc. of sizes ranging from 3 to 20 have been investigated for their ground-state and low-lying geometries, structural stability, bonding characteristics, and in some cases vibrational properties. A way to get insight into the physics of clusters is to dope them with an impurity. A few investigations of an impurity in metal-atom clusters using an *ab initio* molecular-dynamics method have been reported on Na_nMg [9], Li_nAl [10,11] (where a monovalent host is doped with a divalent and a trivalent impurity, respectively). Also the clusters with trivalent host Al and monovalent impurities such as Li and Na have been studied [12,13]. The results are also available on heteroatomic clusters such as alkali-metal-atom–antimony (A_nSb_4) clusters [14], Na_nF_n [15], Na_nK_m [16], etc. These early investigations have revealed that (1) the addition of the impurity atom changes the geometries of small pure clusters, (2) there is an early appearance of nonplanar structures, (3) in some cases the impurity prefers to get trapped inside the cage formed by the host atoms.

In the present work, we study the Na_nAl ($n=1,10$) clusters, which have a trivalent impurity in a monovalent host. We compare and contrast these results with that of (1) Li_nAl [10] clusters where the same trivalent impurity is added in a different monovalent host Li and (2) Na_nMg [9] where a divalent impurity Mg is added in the same monovalent host Na. In the earlier calculations it had been reported that for small Li_nAl clusters, the impurity atom prefers to get trapped inside the cage formed by Li atoms whereas for Na_nMg although the Mg atom gets trapped inside the cage formed by Na atoms, it is not at the center of the cluster.

Our calculations are based on the CPMD technique, which has emerged as one of the most powerful tools for *ab initio* investigations of clusters. However, the conventional CPMD technique using Kohn-Sham orbitals can be computationally very expensive especially for large systems. Recently, we developed and applied a density-based molecular dynamics (DBMD) method that uses approximate kinetic energy functionals based on charge density only. Our investigations show that the DBMD method yields the correct ground state geometries (except for Jahn-Teller distortion) and bond lengths to within 10% of CPMD. This has been verified for many clusters *viz*. small dimers and trimers [11], Li_nAl ($n=1,8$) [11], Na_n ($n=1,8$) [17], Li_n ($n=1,8$) [17], and Al_n ($n=1,8$) [17]. Thus a combination of DBMD and CPMD offers an attractive strategy for obtaining the ground-state geometries of clusters with much less computational effort. In the present work we have followed the same strategy.

Thus we first obtain the ground-state geometries of Na_nAl ($n=1,10$) clusters by employing the full simulated annealing strategy with DBMD and then these structures are further quenched with CPMD using nonlocal pseudopotentials. Thus the final results presented here are obtained with CPMD. In this work CPMD will always mean a Kohn-Sham-orbital–based method and DBMD will mean an approximate density-based method.

In the next section we briefly describe the salient features of DBMD and CPMD along with the relevant numerical details.

II. METHOD AND NUMERICAL DETAILS

Our approach is slightly different in the sense that the DBMD method is used first to scan the configuration space

*Electronic address: ajd@physics.unipune.ernet.in
†Electronic address: vaishali,kanhere@unipune.ernet.in

extensively and the geometry thus obtained is used as input for CPMD. The CPMD method used has been well documented and our implementation is the standard one. Hence a brief account of only DBMD is given here.

The total energy of a system consisting of N_a atoms and N_e interacting electrons, under the influence of an external field due to the nuclear charges at coordinates R_n can be written as a functional of the total electronic charge density $\rho(\mathbf{r})$ as

$$E[\rho,\{R_n\}]=T[\rho]+E_{\rm xc}[\rho]+E_c[\rho] \tag{1}$$

$$+E_{\rm ext}[\rho,\{R_n\}]+E_{ii}(\{R_n\}), \tag{2}$$

where $E_{\rm xc}$ is the exchange correlation energy, E_c is the electron-electron Coulomb interaction energy, $E_{\rm ext}$ is the electron-ion interaction energy and E_{ii} is the ion-ion interaction energy. The first term representing the kinetic energy functional $T[\rho]$ is approximated as

$$T[\rho]=F(N_e)T_{\rm TF}[\rho]+T_W[\rho], \tag{3}$$

where $T_{\rm TF}$ is the Thomas-Fermi term, T_W is the gradient correction given by Weizsacker, and the factor $F(N_e)$ is

$$F(N_e)=\left(1-\frac{2}{N_e}\right)\left(1-\frac{A_1}{N_e^{1/3}}+\frac{A_2}{N_e^{2/3}}\right) \tag{4}$$

with optimized parameter values $A_1=1.314$ and $A_2=0.0021$. This kinetic energy functional is known to describe the response properties of the electron gas well and has yielded very good polarizabilities for various atomic systems. It also provides an excellent representation of the kinetic energy of atoms. The total electronic energy for a fixed geometry of atoms is minimized using the conjugate gradient technique [18] and the geometry minimization has been performed using Car-Parrinello simulated annealing strategy. All the DBMD calculations were performed using only a local part of Bachelet, Hamann, and Schlüter pseudopotentials [19] and the exchange correlation potential of Ceperley-Alder as interpolated by Perdew and Zunger [20]. A periodically repeated unit cell of length 30 a.u. with a $54\times54\times54$ mesh and time step $\Delta t\sim20$ a.u. was used. We have chosen to use the plane-wave expansion on the entire Fourier-transform mesh without any truncation yielding the energy cutoff of 95 Ry.

During the dynamical simulated annealing, the clusters were heated to 600 K and then cooled very slowly to get the ground-state and low-lying energy configurations. In some cases the geometries of the clusters have been confirmed by starting with different initial configurations and then performing a simulated annealing for a few thousand time steps. The geometry thus obtained was taken to be the starting geometry for CPMD and quenched further to get the final ground-state geometry.

In case of CPMD the full nonlocal pseudopotential of Bachelet, Hamann, and Schlüter up to p nonlocality has been used with energy cutoff of 12 Ry. Apart from changes in bond length, symmetries obtained (except for Jahn-Teller distorted systems) are the same as that obtained by DBMD. In addition we have also performed the full simulated annealing study using the CPMD method for Na_6Al and Na_8Al and verified that the ground-state geometries obtained by both methods (DBMD and CPMD) are identical.

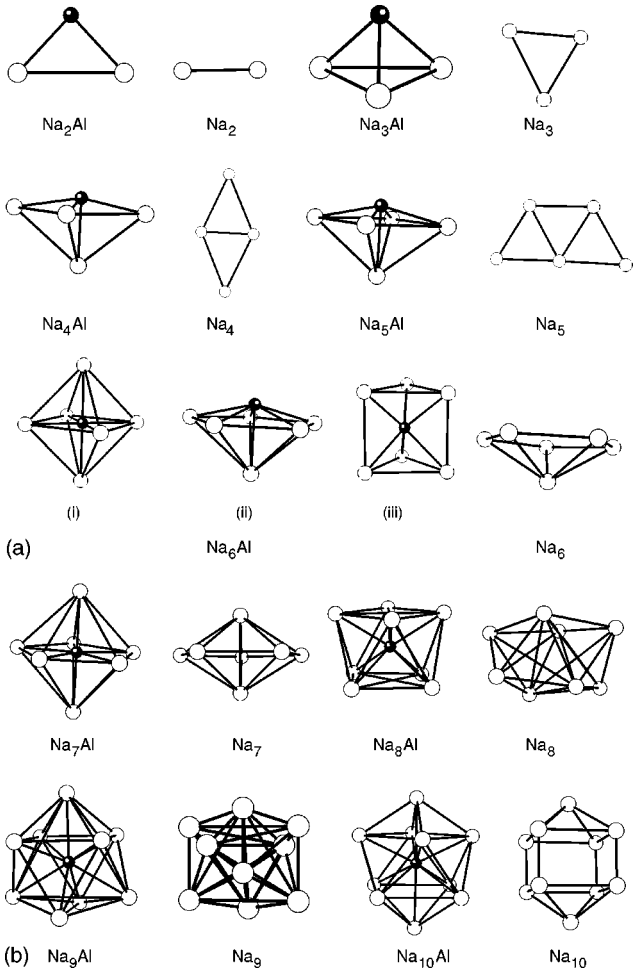

FIG. 1. (a) The ground-state geometries of Na_nAl clusters along with Na_n ($n=2,6$) clusters. (The dark circle represents an Al atom and the white circle a Na atom.) (b) The ground-state geometries of Na_n Al clusters along with Na_n ($n=7,10$) clusters. (The dark circle represents an Al atom and the white circle a Na atom.)

III. RESULTS

The ground-state equilibrium geometries for Na_nAl ($n=2,10$) clusters are shown in Figs. 1(a) and 1(b) where a dark sphere represents the Al impurity. For proper comparison we have also shown the ground-state geometries of Na_n ($n=2,10$) clusters [4]. First, we discuss the general features observed in these clusters and compare the results with homoatomic Na_n clusters wherever appropriate. We will also compare and contrast them with the reported CPMD results for Li_nAl ($n=1,8$) [10] and Na_nMg ($n=6,9$ and 18) [9] clusters.

Figures 1(a) and 1(b) clearly show that for small Na_n ($n<6$) clusters the ground-state geometries change significantly on addition of an Al impurity while for larger clusters the effect of impurity is less pronounced. It is seen that for homoatomic Na_n clusters the ground-state geometries are nonplanar for $n>5$ onwards whereas on addition of an Al impurity, an early appearance of nonplanar ground-state ge-

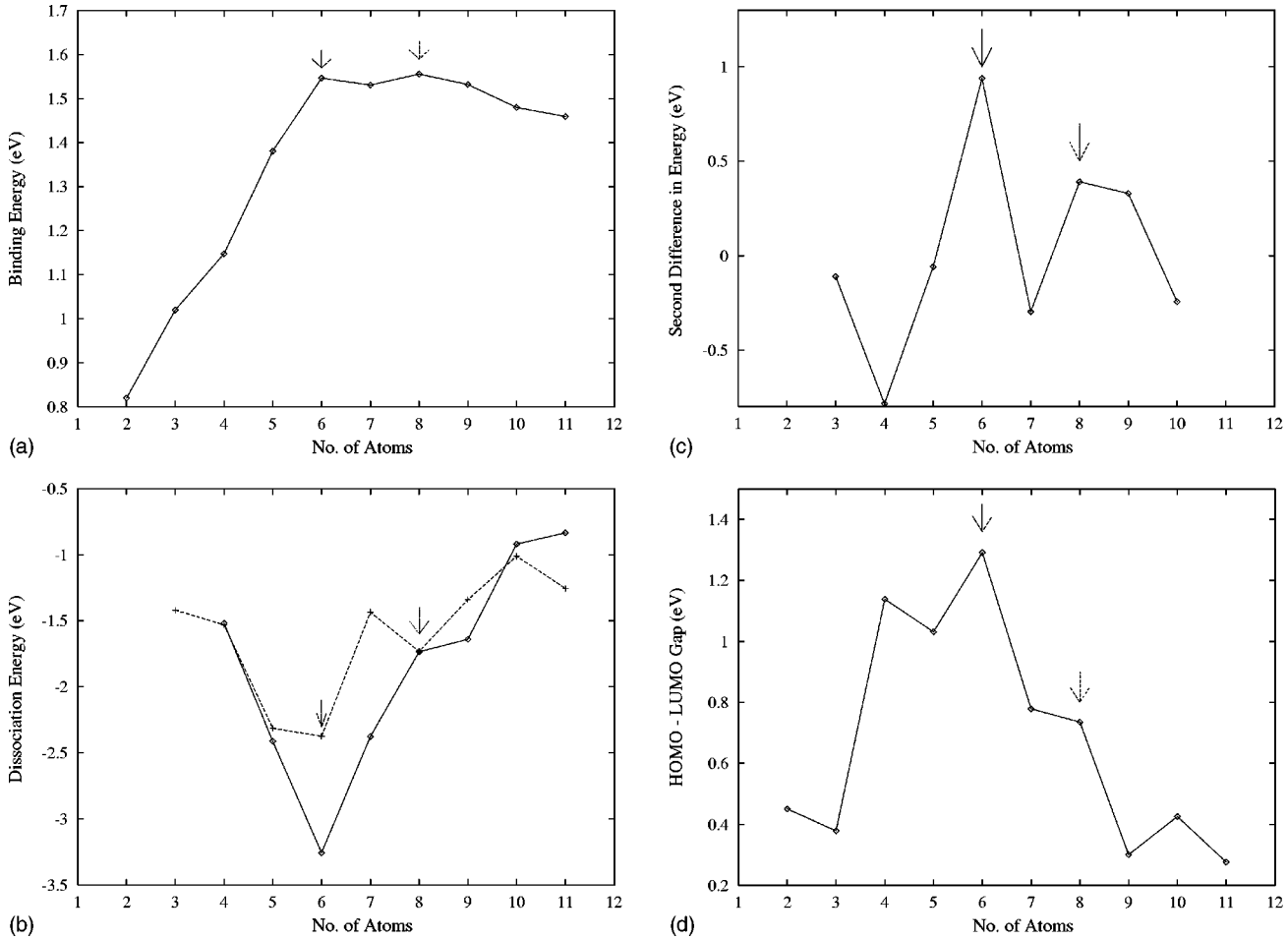

FIG. 2. (a) The binding energy (eV) per atom for the Na_nAl ($n=1,10$) clusters shown as a function of the total number of atoms. (Arrows indicate the stable clusters.) (b) The dissociation energy (eV) for the Na_nAl ($n=1,10$) clusters as a function of the total number of atoms. The dotted curve represents dissociation with respect to a single Na atom and the continuous curve shows dissociation with respect to the Na dimer. (Arrows indicate the stable clusters.) (c) The second difference in energy (eV) for the Na_nAl ($n=1,10$) clusters shown as a function of the total number of atoms. (Arrows indicate the stable clusters.) (d) The HOMO-LUMO gap (eV) for the Na_nAl ($n=1,10$) clusters shown as a function of the total number of atoms. (Arrows indicate the stable clusters.)

ometries ($n=3$ onwards) is observed. According to the spherical jellium model, the nonplanar structure is expected when the p_z orbital gets occupied. Note here that both clusters Na_6 and Na_3Al for which a planar to nonplanar transition occurs are 6-electron systems. In the case of Na_6 [4] the highest occupied level is triply degenerate while for Na_3Al this level splits into singlet having p_z character which is completely filled and two degenerate states having p_x and p_y characters. This level structure makes Na_3Al nonplanar. Thus early appearance of nonplanar structures is related to the p_z orbital of an Al $3p$ electron (hybridized with a Na $3s$ electron) getting occupied in tetrahedral coordination.

Another feature to be noticed is that for $n>5$ the Al atom gets trapped inside the Na cage and is almost at the center of mass of the cluster. This behavior is similar to that observed in Li_nAl [10,11] clusters. However, in the case of Na_nMg [9] it has been observed that the Mg atom does not get trapped for $n\leqslant 9$ [9,21]. The trapping of an impurity atom can be understood on the basis of ionic radii of constituent atoms and the strength of the bond between them. The ionic radius of Na (1.57 Å) is largest among Mg (1.36 Å), Al (1.25 Å), and Li (1.25 Å). From the radii values it is also clear that Al is more easily trapped than Mg inside the Na cage. The trapping is also influenced by the strength of relative bonds involved. It is seen that the Na-Mg bond (0.23 eV) [22] is weaker than the Na-Al bond (0.82 eV) [22] due to the close shell configuration of Mg, which makes it weakly interacting.

In the ground-state NaAl cluster has $C_{\infty v}$ symmetry with bond length between Na-Al as 5.55 a.u. As expected Na_2 Al goes into an isosceles triangle, however, the presence of an Al atom makes the Na_3 Al cluster tetrahedral. Na_4 Al is the first cluster whose geometry differs significantly from a pure Na_4 cluster. Na_4 forms a rhombus (planar geometry), whereas Na_4Al is a pyramid (nonplanar geometry). Again note the difference between Na_5 and Na_5Al clusters. Na_5 is planar with C_{2v} symmetry and Na_5Al is formed by capping the pyramid of Na atoms by Al on the other side of Na_4 plane. Trapping of an Al impurity atom at the center of cluster is first seen for Na_6Al. The Na_6 cluster is the first nonplanar cluster in the case of pure Na clusters where five Na atoms form a pentagon and the remaining Na atom caps this pentagon. Addition of an Al atom to this cluster changes this structure significantly into an octahedron but this octahedral geometry in the case of Na_6 has been demonstrated to be unstable. The ground-state geometry of Na_6Al shown in Fig.

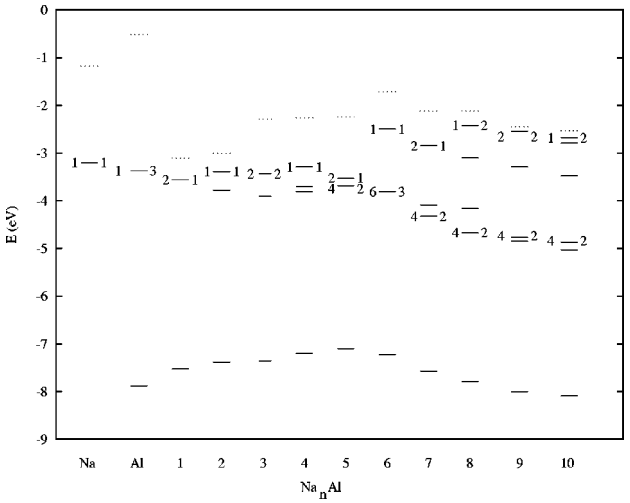

FIG. 3. Eigenvalue spectrum for Na, Al, and Na_nAl ($n=1,10$). (Energies are in eV.) Unoccupied states are shown with dotted lines. For the highest occupied state and the lower occupied degenerate states the number on the right of a state denotes degeneracy while the number on the left denotes total occupancy. All other occupied states have occupancy 2.

1(a)(i) is similar to Li_6Al. However, this geometry is different from that of Na_6Mg. We have also obtained the two low-lying almost degenerate structures of Na_6Al shown in Figs. 1(a)(ii) and 1(a)(iii) with an energy difference of 0.1 eV compared to the ground state. One of these viz., the pentagonal bipyramidal structure shown in Fig. 1(a)(ii) happens to be the ground-state energy structure of Na_6Mg. In Na_7Al, the Al atom prefers to occupy the central position in a pentagonal bipyramid, which is the ground-state geometry of Na_7. In this case Al can be considered as an interstitial impurity in Na_7. The ground state of Na_8 is the dodecahedron. But in the case of Na_8Al, Al gets trapped in the archimedian antiprism, which is one of the low-lying energy structures of Na_8. Thus it seems that the Al impurity stabilizes one of the low-lying energy structures of Na_8. The Na_9Al cluster is very different from Na_9 and is seen to be obtained by capping the Na_8Al structure. $Na_{10}Al$ can also be considered as a case of interstitial impurity since the Al atom gets trapped at the center of ground-state structure of Na_{10}, which is the bicapped antiprism. Finally, we remark that, Li and Na being isoelectronic, Na_nAl and Li_nAl ($n=1,10$) clusters have similar ground-state geometries except for $n=7$, which arises due to the different geometries of Na_7 and Li_7.

The stability of the Na_nAl ($n=1,10$) clusters is discussed on the basis of their energetics. We define the binding energies per atom $E_b[Na_nAl]=(-E[Na_nAl]+nE[Na]+E[Al])/(n+1)$ and the second difference in energy as $\Delta^2E[Na_nAl]=-2E[Na_nAl]+E[Na_{n+1}Al]+E[Na_{n-1}Al]$. The dissociation energy with respect to single Na dissociation is given by $\Delta E[Na_nAl]=E[Na_nAl]-(E[Na_{n-1}Al]+E[Na])$ and with respect to Na dimer dissociation by $\Delta E[Na_nAl]=E[Na_nAl]-(E[Na_{n-2}Al]+E[Na_2])$.

In Fig. 2(a) the binding energy per atom (in eV) is plotted against the total number of atoms in the system. The binding energy shows a monotonic increase with two slight peaks for Na_5Al and Na_7Al, which are 8 and 10 valence electron systems, respectively. It can be noted that with the Na-Al bond being stronger than the Na-Na bond the addition of the Al impurity is favored over the addition of a Na atom. This is also confirmed from the comparison of binding energies of clusters having the same number of total atoms, e.g., NaAl (0.82 eV)— Na_2 (0.71 eV), Na_6Al (1.56 eV)— Na_7 (1.147 eV), and Na_7Al (1.556 eV)— Na_8 (1.216 eV).

In Fig. 2(b) the dissociation energy (in eV) has been plotted against the total number of atoms in the cluster. The dissociation energy has been calculated with respect to two dissociation channels viz., dissociation of a single Na atom (shown by a dotted line in the figure) and dissociation of a Na dimer from the cluster (shown by a continuous line). Note the absence of a clear odd-even pattern as was also seen in case of Li_nAl [10] clusters. A single Na atom dissociation channel shows the minima for Na_5Al and Na_7Al. The com-

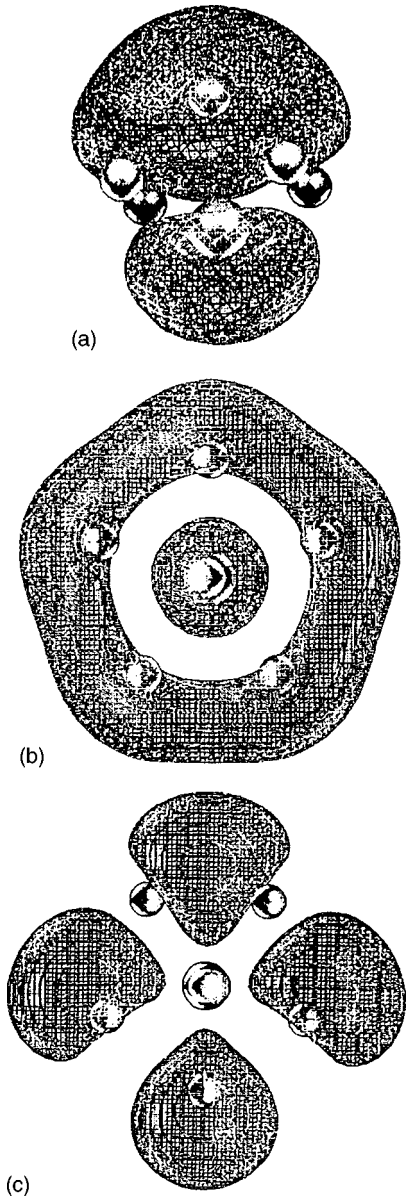

FIG. 4. (a) Isodensity surface corresponding to the highest occupied state for the Na_5Al cluster. (b) Isodensity surface corresponding to the highest occupied state for the Na_7Al cluster. (c) Isodensity surface corresponding to the lowest unoccupied state for the Na_7Al cluster.

TABLE I. The total number of electrons in the system (N_e), the symmetry, the minimum bond lengths (in a.u.) obtained using CPMD as well as DBMD between Na-Al and Na-Na along with eccentricity parameter (obtained using CPMD) for Na_nAl ($n=1,10$) clusters.

System	N_e	Symmetry	Bond length (a.u.)				η
			CPMD		DBMD		
			Na-Al	Na-Na	Na-Al	Na-Na	
NaAl	4	$C_{\infty v}$	5.55		4.85		1.0000
Na_2Al	5	C_{2v}	2×5.57	5.87	2×4.81	6.51	0.2830
Na_3Al [a]	6	C_{3v}	2×5.44	6.00	3×4.84	6.31	
			5.46				
Na_4Al [a]	7	C_{3v}	2×5.41	5.77	4×4.89	6.20	0.3430
			2×5.22				
Na_5Al	8	C_{4v}	4×5.13	5.97	4×4.88	6.11	0.1445
			5.54		4.97		
Na_6Al	9	O_h	6×5.00	7.02	6×4.84	6.80	0.0324
Na_7Al	10	D_{5h}	2×5.02	6.12	2×4.85	5.87	0.0480
			5×5.22		5×5.00		
Na_8Al	11	D_{4d}	8×5.29	6.14	8×5.05	6.05	0.0815
Na_9Al [a]	12	C_{3v}	6×5.35	6.18	6×5.12	5.86	0.0120
			2×5.49		3×5.23		
			5.52				
$Na_{10}Al$ [a]	13	D_{4d}	8×5.43	5.99	8×5.23	5.64	0.1010
			6.05, 6.10		2×5.45		

[a]Jahn-Teller distorted systems. (For these systems symmetries of corresponding undistorted symmetric structures are given.)

parison of the dissociation energies corresponding to these two channels clearly shows that Na_6Al and Na_8Al prefer dissociation of Na since this dissociation leads to Na_5Al and Na_7Al clusters, respectively, which are more stable. But in the case of Na_9Al, rather than Na dissociation which results in the formation of Na_8Al, the dissociation of Na_2 is favored since it produces one of the stable clusters viz., Na_7Al.

In Fig. 2(c) the second difference in energy (in eV) is plotted against the total number of atoms in the cluster. The figure shows peaks at Na_5Al and Na_7Al clusters confirming their stability. In Fig. 2(d) the difference in the highest occupied and the lowest unoccupied molecular orbital energies (HOMO-LUMO gap in eV) are plotted against the total number of atoms in the system. Note that the gap is highest for Na_5Al ($8e^-$ system) indicating it to be the most stable and for Na_7Al although the gap is reduced it is still significant and is of the order of 0.74 eV. The figure also shows a sudden jump at Na_3Al due to the transition from planar to nonplanar structure.

Now we will discuss the stability of 8 and 10 electron systems on the basis of the energy level diagram shown in Fig. 3 and spherical jellium model [23]. In the Fig. 3 we have shown the energy levels for all the clusters studied along with Na and Al atoms. It is clear from the figure that the lowest eigenvalue (originating from Al $3s$ level) is well separated from higher-lying ones. Figure 3 clearly shows the electronic cluster shell filling for 8 electrons with a sizable HOMO-LUMO gap. Further the isodensity surface corresponding to the highest occupied level [see Fig. 4(a) where hollow spheres represent the atoms] for Na_5Al shows a marked localized character. These characteristics are similar to Li_5Al [10]. Therefore we believe that the stability of this cluster is influenced by the localized atomic levels and thus this 8-electron system is stable mainly because of closing of Al $3p$ manifold. Further noting the eigenspectrum beyond Na_5Al, which is similar to Li_nAl [10] system, it may be possible to describe the stability of clusters for $n>5$ using the description of a spherical jellium model. In this model it is assumed that the clusters are spherical and the ionic charge is distributed homogeneously. The calculated electronic shell structure orders as $1s^2$, $1p^6$, $1d^{10}$, $2s^2$, $2p^6$, $1f^{14}$, etc. So when the number of valence electrons in the cluster is just enough to complete one of the electronic shells, the corresponding cluster exhibits enhanced stability. In the case of alkali-metal clusters [24] the first-principle calculation has confirmed this picture. However, for systems with trivalent atoms like Al this is not necessarily so. In the present case it appears that the $1d$ and $2s$ levels are reversed ($2s$ has lower energy than $1d$). This feature is also confirmed from the eigenspectrum (see Fig. 3) and the isodensity surface corresponding to the highest occupied level shown in Fig. 4(b) (where hollow spheres represent the atoms) and the lowest unoccupied level shown in Fig. 4(c) (where hollow spheres represent the atoms) for a Na_7Al cluster. The charge density in Fig. 4(b) shows a dominant s character while Fig. 4(c) shows a dominant $d(x^2-y^2)$ character. It is also seen that there is no significant degree of $2s$-$1d$ mixing. This may be contrasted with a Li_7Al [10] cluster, which is not stable due to the significant hybridization between s and d states. Thus the closing of a $2s$ shell makes the Na_7Al ($10e^-$) cluster stable.

Different parameters viz. total number of electrons (N_e), symmetry, distances between Al and Na atoms, shortest distance between Na-Na (for CPMD as well as DBMD), and eccentricity are summarized in Table I. The eccentricity parameter η is defined as $\eta = 1 - I_{\min}/I_{\text{av}}$, where $I_{\min}$ is the minimum value of the moment of inertia and I_{av} is the average value of the moment of inertia. If η is small, it indicates the cluster to be spherically symmetric. In general, η decreases as the number of atoms in the cluster increase, describing the isotropic distribution of atoms around the center. It is gratifying to note that DBMD bond lengths are within 10% of CPMD. The comparison of Na-Al bond lengths obtained using CPMD and DBMD clearly shows Jahn-Teller distortion for Na_3Al, Na_4Al, Na_9Al, and $Na_{10}Al$ clusters.

IV. CONCLUSIONS

In the present work, we have obtained the ground-state geometries of Na_nAl ($n=1,10$) clusters using *ab initio* molecular dynamics method and compared them with Li_nAl and Na_nMg clusters wherever possible. Our results show an early appearance of three-dimensional structures and the trapping of Al impurity inside the cage of Na atoms for $n \geqslant 6$ similar to the trend observed in case of Li_nAl clusters but different from Na_nMg clusters. In some cases the Al atom acts as an interstitial impurity and in some cases it stabilizes one of the corresponding low-lying geometries. The stability analysis predicts Na_5Al and Na_7Al to be the stable clusters. The HOMO-LUMO gap and dissociation channels corresponding to dissociation of Na and Na_2 dissociation confirm the stability of these clusters.

ACKNOWLEDGMENTS

We gratefully acknowledge the financial assistance from CSIR (New Delhi) and Department of Science and Technology. One of us (A.D.) also acknowledges partial financial assistance from the Government of Maharashtra. It is our pleasure to acknowledge Vijay Kumar for useful discussions.

[1] *Physics and Chemistry of Finite Systems: From Clusters to Crystals*, edited by P. Jena, S. N. Khanna, and B. K. Rao (Kluwer Academic, Dordrecht, Netherlands, 1992), Vols. 1 and 2.

[2] *Clusters and Nanostructured Materials*, edited by P. Jena and S. N. Behera (Nova Science Publishers, Inc., New York, 1996).

[3] M. C. Payne, M. P. Teter, D. C. Allan, T. A. Arias, and J. D. Joannopoulos, Rev. Mod. Phys. **64**, 1045 (1992).

[4] J. L. Martins, J. Buttet, and R. Car, Phys. Rev. B **31**, 1804 (1985); U. Rothlisberger and W. Andreoni, J. Chem. Phys. **94**, 8129 (1991).

[5] V. Kumar and R. Car, Phys. Rev. B **44**, 8243 (1991).

[6] H. P. Cheng, R. S. Berry, and R. L. Whetten, Phys. Rev. B **43**, 10 647 (1991).

[7] G. Seifert and R. O. Jones, Z. Phys. D **26**, 349 (1993).

[8] D. Hohl, R. O. Jones, R. Car, and M. Parrinello, Chem. Phys. Lett. **139**, 540 (1987).

[9] U. Rothlisberger and W. Andreoni, Chem. Phys. Lett. **198**, 478 (1992).

[10] H. Cheng, R. Barnett, and Uzi Landman, Phys. Rev. B **48**, 1820 (1993).

[11] D. Nehete, V. Shah, and D. G. Kanhere, Phys. Rev. B **53**, 2126 (1996).

[12] C. Majumder, G. P. Das, S. K. Kulshrestha, V. Shah, and D. G. Kanhere, Chem. Phys. Lett. **261**, 515 (1996).

[13] H. Matsuzawa, T. Hanawa, K. Suzuki, and S. Iwata, Bull. Chem. Soc. Jpn. **65**, 2578 (1992).

[14] F. Hagelberg, S. Neeser, N. Sahoo, and T. P. Das, Phys. Rev. A **50**, 557 (1994).

[15] J. Giraud-Girard and D. Maynau, Z. Phys. D **32**, 249 (1994).

[16] A. Bol, G. Martin, J. M. Lopez, and J. A. Alonso, Z. Phys. D **28**, 311 (1993).

[17] D. Nehete, V. Shah, and D. G. Kanhere (unpublished); V. Shah, Ph.D. thesis, University of Pune, 1997 (unpublished).

[18] W. H. Press, B. P. Flannery, S. A. Teukolsky, and W. T. Vetterling, *Numerical Recipes* (Cambridge University Press, Cambridge, 1987).

[19] G. B. Bachelet, D. R. Hamann, and M. Schluter, Phys. Rev. B **26**, 4199 (1982). Although it is possible to incorporate the nonlocality in DBMD as an *ad hoc* prescription, a correct formulation is not yet available.

[20] J. P. Perdew and A. Zunger, Phys. Rev. B **23**, 5048 (1981).

[21] Our preliminary CPMD results on Na_nMg ($n=1,12$) (unpublished) indicate that Mg gets trapped for $n \geqslant 10$.

[22] The strength of the bond is taken to be the binding energy of corresponding diatomic system.

[23] M. Brack, Rev. Mod. Phys. **65**, 677 (1993).

[24] W. D. Knight, K. Clemenger, W. A. de Heer, W. A. Saunders, M.-Y. Chou, and M. L. Cohen, Phys. Rev. Lett. **52**, 2141 (1984).